Polymer Journal (2012) 44, 620–624

www.nature.com/pj

ORIGINAL ARTICLE

Fabrication of novel core-shell microspheres consisting of single-walled carbon nanotubes and $CaCO_3$ through biomimetic mineralization

Tomoyuki Tajima, Akira Tsutsui, Tatsuo Fujii, Jun Takada and Yutaka Takaguchi

Calcium carbonate ($CaCO_3$) in the presence of single-walled carbon nanotube (SWCNT) /fullerodendron supramolecular nanocomposites was crystallized with a CO_2 diffusion method under ambient conditions and in aqueous environments to produce monodisperse spherical SWCNT/$CaCO_3$ hybrids with a core-shell structure. The crystals nucleate at the carboxyl groups on the surface of the SWCNT/fullerodendron supramolecular nanocomposites grow around a spherical scaffold consisting of the SWCNTs, and finally form spherical calcite crystals embedded with and covered by the SWCNTs. Owing to of the phase transition from vaterite to calcite through a solvent-mediated process, the morphology of the microspheres is unique; the shell is primarily composed of calcite crystals of $CaCO_3$, and a greater amount of SWCNTs is embedded in the core moiety.
Polymer Journal (2012) **44,** 620–624; doi:10.1038/pj.2012.36; published online 18 April 2012

Keywords: biomineralization; calcium carbonate; carbon nanotubes; core-shell structure; dendrimer; fullerene; nanohybrid

INTRODUCTION

Nanohybrids of single-walled carbon nanotubes (SWCNTs) and inorganic materials are a new class of functional materials that have attracted tremendous interest in recent years because of their exceptional optical, mechanical, electrical and thermal properties.[1–12] A structure with hierarchical organization and a complex shape that is based on SWCNTs is attractive and intriguing because the functionality of the materials is highly dependent on their nano/meso-architectures. Recently, we have reported the fabrication of SWCNT/fullerodendron/SiO_2 coaxial nanohybrids via sol−gel polycondensation of tetraethoxysilane on the surface of SWCNT/fullerodendron supramolecular nanocomposites.[13] Because their coaxial structure provides a hierarchical photofunctional surface, SWCNT/fullerodendron/SiO_2 nanohybrids exhibit high photocatalytic activity ($\Phi = 0.31$) for the evolution of hydrogen from water under irradiation with visible light (450 nm). In addition, calcium carbonate ($CaCO_3$) is one of the major constituents of many biominerals that possess highly controlled hierarchical and complex structures, which are organic/inorganic hybrids that are produced in living organisms.[14] Inspired by biomineralization, a wide range of organic additives and templates have been utilized in $CaCO_3$ crystallization to facilitate biomimetic morphological control of the crystals.[15–22] For instance, Kato *et al.*[17] have described macromolecular templates for the formation of organic/inorganic hybrid structures. Of these organic macromolecules that facilitate biomimetic composite formation, dendritic macromolecules are currently of considerable interest[23–28] because their regular and highly branched three-dimensional architectures are good candidates for the study of crystal nucleation and the growth of $CaCO_3$. Using anthryl dendron, in which the focal point is anthracene and terminals are carboxyl groups, we incorporated anthracene into vaterite $CaCO_3$ crystals.[29] Interestingly, photodimerization of the anthracene units proceeded within the anthryl dendron/$CaCO_3$ nanohybrids. Furthermore, we have reported fullerodendron/$CaCO_3$ nanohybrids, in which fullerodendrons had a crucial role in both the controlled crystallization of unstable vaterite and the singlet oxygen photosensitizing properties.[30] When considering the photofunctional hybrid materials formed under mild conditions, the synthesis of SWCNT/$CaCO_3$ hybrids using biomimetic mineralization is of great interest.[31–33] However, only a few examples of the mineralization of $CaCO_3$ using SWCNTs have been described in the literature,[31,33] and these have used the covalent sidewall functionalization of SWCNTs to produce an effective template for hybridization.[34–39] Thus, we investigated the synthesis of SWCNT/$CaCO_3$ hybrids by utilizing SWCNT/fullerodendron supramolecular nanocomposites,[13] that is, non-covalent functionalized SWCNTs,[40–44] which possess many carboxyl groups on the surface (Chart 1). This report describes the fabrication of core-shell microspheres consisting of $CaCO_3$ and SWCNTs through biomimetic mineralization under ambient conditions in an aqueous environment. The mechanism of formation for this unique structure is also discussed.

Department of Chemistry, Graduate School of Environmental Science, Okayama University, Okayama, Japan
Correspondence: Professor Y Takaguchi, Graduate School of Environmental Science, Okayama University, Tsushima-Naka 2-1-1, Kita-ku, Okayama 700-8530, Japan.
E-mail: yutaka@cc.okayama-u.ac.jp
Received 25 January 2012; revised 13 February 2012; accepted 14 February 2012; published online 18 April 2012

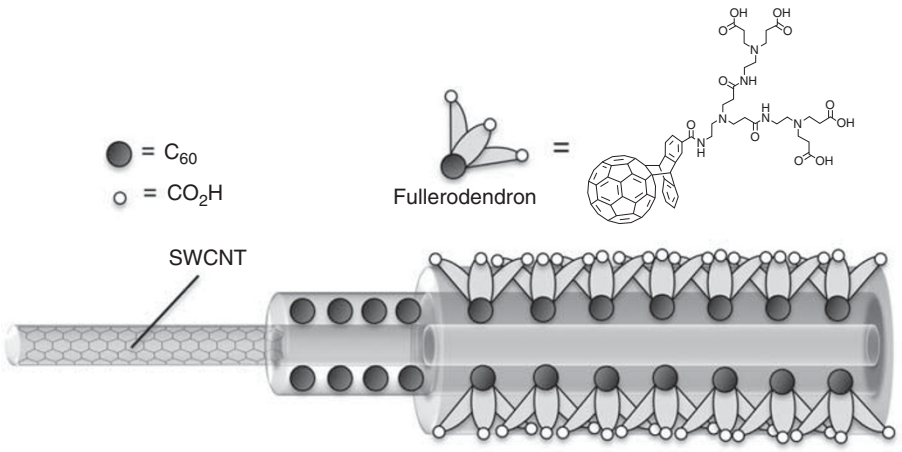

Chart 1 Schematic illustration of the SWCNT/fullerodendron supramolecular nanocomposite.

EXPERIMENTAL PROCEDURE

Instruments

Fourier transform infrared spectroscopy (FT-IR) analysis was performed with a Shimadzu IRAffinity-1 infrared spectrometer (Shimadzu, Kyoto, Japan). Scanning electron microscopy (SEM) was recorded on a Hitachi S-3500 N (Hitachi, Tokyo, Japan). X-ray diffraction patterns were measured with CuKα radiation using a Rigaku RAD (Rigaku, Tokyo, Japan) at room temperature. Raman spectra were obtained with a HORIBA Jobin Yvon XploRA Raman spectrometer (HORIBA, Kyoto, Japan) using laser excitation at wavelengths of 532 and 785 nm. Thermogravimetric analyses were performed with a Shimadzu DTG-60 at 10 °C per min under air. SWCNTs (HiPco) were purchased from Carbon Nanotechnologies, Inc. (Houston, TX, USA) SWCNTs (CoMoCAT) were purchased from SouthWest Nano Technologies, Inc. (Norman, OK, USA). Ammonium carbonate (Kanto Kagaku Co., Ltd, Tokyo, Japan), calcium chloride (Nacarai Tesque, Kyoto, Japan) and distilled water were used without further purification. All other reagents were obtained from Kanto Kagaku Co., Ltd, Sigma-Aldrich Japan, Co. (Tokyo, Japan) and Tokyo Kasei Co., Ltd. (Tokyo, Japan). All chemicals were used as received. Fullerodendron was prepared according to the reported procedure.[45]

Formation of SWCNT/fullerodendron supramolecular nanocomposites

In a typical experiment, SWCNTs (HiPco: 1.0 mg) were placed in a H_2O solution (10 ml, 10.0 mM) of fullerodendron (164 mg, 0.1 mmol) and sonicated with a bath-type ultrasonifier (ULTRASONIC CLEANER vs-D100, 110 W, 24 kHz, As One, Co., Osaka, Japan) at a temperature below 25 °C for 1 h.[46] After the suspension was centrifuged at 3000 *g* for 30 min (TOMY LC-200, Tokyo, Japan), a black-colored supernatant solution was collected. The solution was used in further experiments as a solution of SWCNT/fullerodendron supramolecular nanocomposites.

Crystallization of $CaCO_3$ in the presence of SWCNT/fullerodendron nanocomposites

The mineralization experiments were performed by a slow carbonate diffusion method (Supplementary Figure S1).[47] Typically, a stock solution of SWCNT/fullerodendron supramolecular nanocomposites (0.84 ml) was diluted with water (4.2 ml), and the mixture, after adjusting the pH to 10.0, the mixture was added to the sample bottle (8 ml). An aqueous solution (0.8 ml) of calcium chloride (0.05 M) was added at room temperature while stirring gently. The sample bottle was then placed in a closed desiccator (3000 ml) containing crushed ammonium carbonate (20 g, 0.21 mol). Carbon dioxide was introduced to the solution via vapor diffusion. The solution was maintained at 25 °C for 2 days. The obtained precipitate was decanted with distilled water and acetone several times. After drying in vacuo at room temperature, the SWCNT/$CaCO_3$ hybrids were obtained.

RESULTS AND DISCUSSION

The SWCNT/$CaCO_3$ hybrids were prepared by the crystallization of $CaCO_3$ in the presence of the SWCNT/fullerodendron supramolecular nanocomposites using a CO_2 diffusion method (Supplementary Figure S1).[47] An aqueous solution of calcium chloride was added to a solution of SWCNT/fullerodendron supramolecular nanocomposites. After stirring gently for a few minutes at room temperature, the solution was placed in a closed desiccator containing crushed ammonium carbonate. The CO_2 was evolved in a closed desiccator. The solution was maintained at 25 °C for 2 days. The obtained precipitate was decanted with distilled water and acetone several times. The SWCNT/$CaCO_3$ hybrids were obtained as brown crystals (Supplementary Figure S2).

Figure 1 shows the SEM images of the SWCNT/$CaCO_3$ hybrids that were formed in the presence of the SWCNT/fullerodendron supramolecular nanocomposites. Monodisperse and spherical $CaCO_3$ particles with diameters of 10 −15 μm were observed (Figure 1a). The $CaCO_3$ particles can be handled in air for at least a few months. The magnified SEM image showed that the surface is composed of rhombohedral subunits with a size of 1 μm (Figure 1b). White mesh-like lines were observed on the surface of the subunits in the high-resolution image (Figure 1c). Nanotubes are known to be highly visible as bright fibers because of their charging phenomena in the SEM images.[48] The fine lines on the surface of the hybrids were most likely SWCNTs. Interestingly, the fractured particles of the SWCNT/$CaCO_3$ hybrids clearly revealed a core-shell structure (Figure 1d). The diameter of the inner sphere was measured at 8 −10 μm, and the shell thickness was estimated to be 2 −5 μm. The inner sphere had a corn cob-like morphology, which is completely different from the morphology of the corn-like outer layer.

The crystal phase of the spherical $CaCO_3$ hybrids was determined by X-ray diffraction and FT-IR measurements. The X-ray diffraction patterns exhibited reflections at 0.304, 0.289, 0.250, 0.229, 0.209, 0.192, 0.188, and 0.160 nm, which can be assigned to the (104), (006), (110), (113), (202), (024), (116) and (122) reflections of calcite, respectively (Figure 2a). (JCPDS ASTM Card nos. 05-0586) In the FT-IR spectrum, three bands were observed at 713, 874 and 1424 cm^{-1}, which are characteristic bands of calcite (Figure 2b).[49] This result was in marked contrast to our previous report demonstrating that vaterite was obtained using fullerodendron ([fullerodendron] = 4.43 mM)[30] because the concentration of fullerodendron was very low ([fullerodendron] = 0.121 mM) in this experiment.

To elucidate the existence of SWCNTs in the spherical $CaCO_3$ hybrids, the $CaCO_3$ crystal component of the shell was removed by treatment with hydrochloric acid.[33] The rhombohedral subunits were completely dissolved in hydrochloric acid, and a reasonable amount of SWCNTs was observed on the surface through SEM (Supplementary Figure S3). The existence of SWCNTs in the hybrids was also confirmed by the Raman spectrum (Supplementary Figure S4).[50] The most intense band (at $\sim$1588 cm^{-1}) was assigned to the graphite-like band (G-band) of the SWCNTs. The second feature possessed a frequency between 1250 and 1450 cm^{-1} and is a disorder-induced Raman band, denoted as a D-band, of SWCNTs. The very small intensity of the D-band indicates that the SWCNTs exist in the composites without any substantial damage. The low frequency features (100–300 cm^{-1}) show the radial breathing mode. These results strongly indicate that the spherical $CaCO_3$ hybrids contain SWCNTs.

The temperature-dependent decomposition of the SWCNT/$CaCO_3$ hybrids was monitored with thermogravimetric analysis (Figure 3). Weight loss (1.6% (w/w)) in the range of 100–200 °C is considered as water loss. A larger weight loss (5.6% (w/w)) caused by the decomposition of the organic parts and C_{60} was observed in the range of 200–400 °C. Weight loss (1.5% (w/w)) in the range of 400–650 °C is considered to result from decomposition of the SWCNT parts. The most significant weight loss occurred in the temperature range of 650–750 °C and is attributed to the decomposition of $CaCO_3$ to CaO.[51–53] The weight loss was 41.5% (w/w), which is in good agreement with the theoretical loss of 40.2% caused by the release of carbon dioxide. Supplementary Figure S5 shows photographs of the hybrids after the thermal treatment at various temperatures. The color of original SWCNT/$CaCO_3$ hybrids changed from brown to black and from black to colorless at 500 °C and 700 °C, respectively, which agrees with the thermogravimetric analysis results.

To clarify the abundance distribution of SWCNTs in the spherical $CaCO_3$ nanohybrid, the SWCNTs were removed by calcination in an air flow at 800 °C for 3 h. Although the spherical morphology of the particles was maintained as shown in Supplementary Figure S6a, the rhombohedral subunits composing the shell of $CaCO_3$ hybrids were segmentalized into tiny nanostructures (Supplementary Figure S6b). Furthermore, a cross section of the microsphere of the calcinated samples revealed a core-shell structure similar to that observed before calcination (Supplementary Figure S6c). The core of the $CaCO_3$ hybrids was also changed into nanosegments with a hollow space in the middle (Supplementary Figure S6d). Drastic changes to the morphology after the calcination treatment occurred as the result of both removing SWCNTs from the hybrid and the conversion of $CaCO_3$ to calcium oxide, which was confirmed by the IR spectra (Supplementary Figure S7). When comparing the morphologies before and after the calcination, a larger amount of SWCNTs was embedded in the core moiety than in the shell moiety of the spherical $CaCO_3$ hybrids.

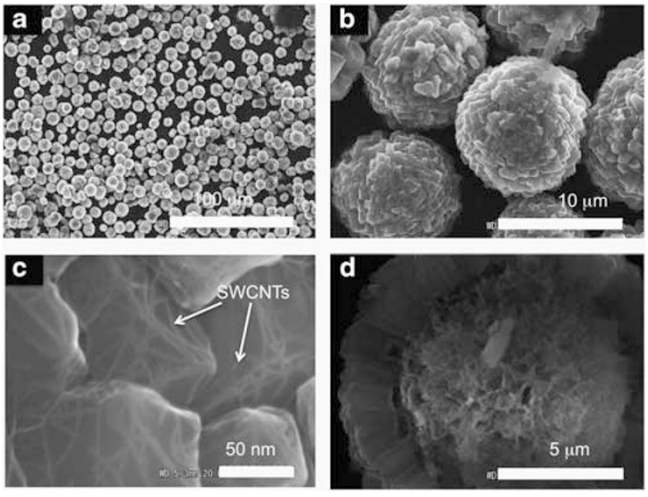

Figure 1 (**a** and **b**) SEM images of SWCNT/$CaCO_3$ hybrids formed in the presence of SWCNT/fullerodendron supramolecular nanocomposites, (**c**) magnified SEM image of the surface of the hybrids and (**d**) a cross-section of the hybrids.

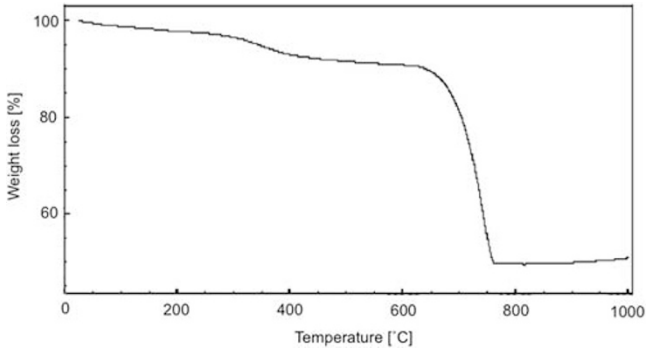

Figure 3 Thermogravimetric analysis plot of the SWCNT/$CaCO_3$ hybrids. SWCNT/$CaCO_3$ hybrids (0.8 mg) were loaded in a Pt pan and heated from ambient temperature to 1000 °C with a heating rate of 10 °C per min under air flow.

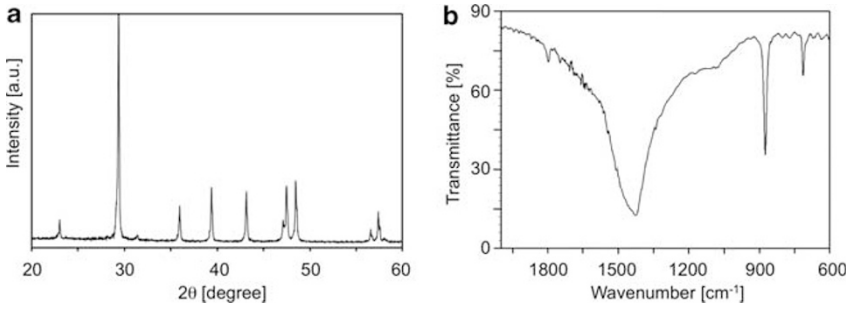

Figure 2 (**a**) X-ray diffraction pattern of the spherical SWCNT/$CaCO_3$ hybrids. The characteristic refection for calcite (*d*-spacing/2θ peak: 3.04 Å/29.4° corresponding to *hkl*: 104). (**b**) FT-IR spectrum of SWCNT/$CaCO_3$ hybrids.

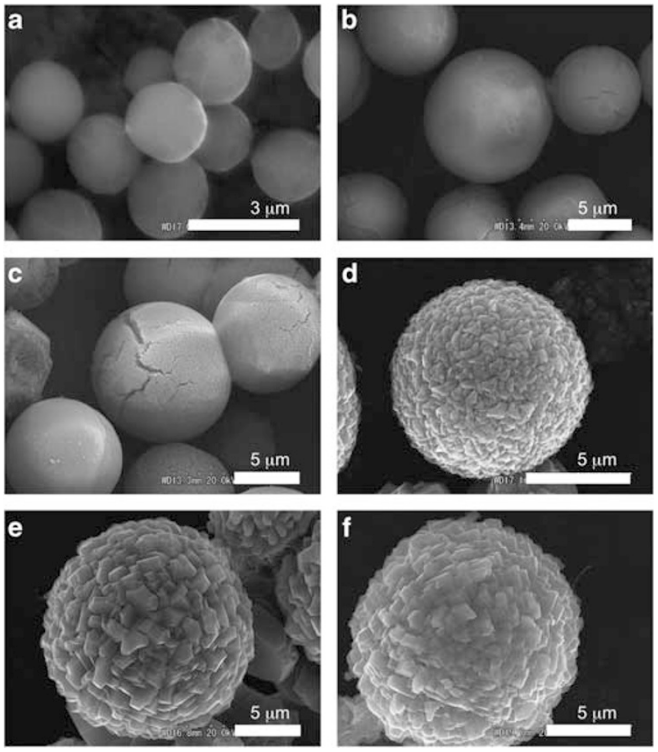

Figure 4 SEM images of SWCNT/$CaCO_3$ hybrids with different crystallization time. (**a**) 0.5 h; (**b**) 1 h; (**c**) 10 h; (**d**) 24 h; (**e**) 36 h and (**f**) 48 h.

To investigate the formation processes of the $CaCO_3$ hybrids in the presence of SWCNT/fullerodendrimer supramolecular nanocomposites, we obtained hybrids that were harvested after different crystallization times (0.5, 1, 10, 24, 36 and 48 h). The SEM image showed spherical $CaCO_3$ hybrids posessing a smooth surface at 0.5 h (Figure 4a). As the reaction time increased from 0.5 to 1.0 h, the spherical particle size obviously increased from 2 to 10 μm while retaining a smooth surface (Figure 4a and b). After 10 h, some cracks were observed on the spherical particles (Figure 4c). After >24 h of crystallization, spherules with rhombohedral subunits began to appear (Figure 4d). A sequence of morphological transitions was completed within 2 days (Figure 4f). These results are further confirmed by FT-IR, as shown in Supplementary Figure S8. At the first stage (1.0 h) of the crystallization of $CaCO_3$, the FT-IR spectrum of the hybrids showed four vibration bands at 1491, 1089, 876 and 750 cm^{-1}, indicating the formation of vaterite,[49] although the typical calcite peak (713 cm^{-1}) was barely detectable. By contrast, after 48 h of crystallization, all of the bands for the typical vaterite phase had disappeared, and new peaks were observed at 713 and 874 cm^{-1}, which were assigned to calcite. These results indicated that the phase transition from vaterite to calcite induced the formation of the core-shell structure of the hybrids.

Figure 5 shows a plausible mechanism for the formation of the core-shell microsphere of the SWCNT/$CaCO_3$ hybrids. The carboxyl groups on the surface of the SWCNT/fullerodendron supramolecular nanocomposites coordinate with the Ca^{2+} ions and provide nucleation sites as shown in Figure 5a. Subsequently, the SWCNT/fullerodendron supramolecular nanocomposites function as a spherical scaffold for the mineralization of $CaCO_3$ (Figure 5b). Subsequent growth of the nuclei stabilized by the scaffold forms the spherical vaterite crystal as shown in Figure 5c. As a consequence of crystal growth, the surface of the metastable vaterite crystals cannot be effectively covered by the scaffold. Under the general conditions of the biomineralization of $CaCO_3$, the metastable vaterite phase generally forms first and then is transformed into the thermodynamically stable calcite through a solvent-mediated mechanism. Hence, the appearance of the uncovered surface of the vaterite triggers the phase transition from vaterite to calcite (Figure 5d). After the phase transition via a solvent-mediated mechanism, which includes the dissolution of vaterite and the subsequent nucleation of calcite, the particular core-shell structure of the hybrids is formed as shown in Figure 5e.

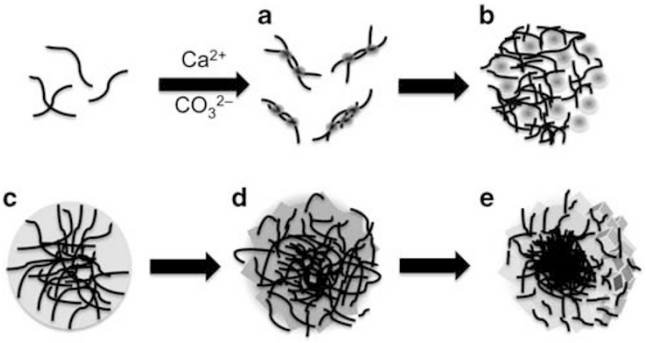

Figure 5 Schematic illustrations for the growth mechanism of the core-shell structure of the SWCNT/$CaCO_3$ hybrids.

To evaluate the generality of our finding, a similar experiment using different SWCNTs produced with the CoMoCAT method,[54] instead of with HiPco tubes, was performed. The SWCNTs (CoMoCAT) have a remarkably narrow distribution of tube diameters (0.75–0.92 nm) compared with those of HiPco (0.83–1.2 nm). Despite the different characters of the SWCNTs, the morphology obtained with the SWCNT/$CaCO_3$ hybrids was identical to that of core-shell microspheres, as confirmed by SEM observation (Supplementary Figure S9).

CONCLUSION

The results described herein show the first example of a core-shell microsphere based on SWCNTs and $CaCO_3$ (calcite). The unique morphology was controlled by SWCNT/fullerodendron supramolecular nanocomposites, which provide the nucleation sites and function as a spherical scaffold for the $CaCO_3$ crystallization process. Owing to their controlled meso-architecture, SWCNT/$CaCO_3$ hybrids have a multitude of potential applications, including as photocatalysts, adsorbents and controlled-release dosage forms of medication. Although there are no reports on the synthesis of SWCNT/$CaCO_3$ hybrids using noncovalently functionalized SWCNTs, the fullerodendron functions as effective 'glue' between the SWCNTs and $CaCO_3$ crystal and enables the facile formation of SWCNT/$CaCO_3$ hybrids. Further work is in progress to explore the fabrication of SWCNT/inorganic hybrids through biomimetic mineralization.

ACKNOWLEDGEMENTS

This work was partially supported by a Grant-in-Aid for Scientific Research (no. 23107522; YT) on Innovative Areas of 'Fusion Materials' (no. 2206) from the Ministry of Education, Culture, Sports, Science and Technology and by a Grant-in-Aid for Scientific Research for Young Scientists (B, no. 23750041; TT) from the Japan Society of the Promotion of Science.

1 Eder, D. Carbon nanotube-inorganic hybrids. *Chem. Rev.* **110,** 1348–1385 (2010).
2 Zhang, W.-D., Xu, B. & Jiang, L.-C. Functional hybrid materials based on carbon nanotubes and metal oxides. *J. Mater. Chem.* **20,** 6383–6391 (2010).
3 Li, X., Qin, Y., Picraux, S. T. & Guo, Z.-X. Noncovalent assembly of carbon nanotube-inorganic hybrids. *J. Mater. Chem.* **21,** 7527–7547 (2011).
4 Krissanasaeranee, M., Wongkasemjit, S., Cheetham, A. K. & Eder, D. Complex carbon nanotube-inorganic hybrid materials as next-generation photocatalysts. *Chem. Phys. Lett.* **496,** 133–138 (2010).
5 Chen, Y., Zhang, T. H., Gan, C. H. & Yu, G. Wear studies of hydroxyapatite composite coating reinforced by carbon nanotubes. *Carbon* **45,** 998–1004 (2007).
6 Zheng, S.-F., Hu, J.-S., Zhong, L.-S., Song, W.-G., Wan, L.-J. & Guo, Y.-G. Introducing dual functional CNT networks into CuO nanomicrospheres toward superior electrode materials for lithium-ion batteries. *Chem. Mater.* **20,** 3617–3622 (2008).
7 Kim, T., Mo, Y. H., Nahm, K. S. & Oh, S. M. Carbon nanotubes (CNTs) as a buffer layer in silicon/CNTs composite electrodes for lithium secondary batteries. *J. Power Sources* **162,** 1275–1281 (2006).
8 Shekhar, C., Giri, R., Malik, S. K. & Srivastava, O. N. Improved critical current density of MgB_2–carbon nanotubes (CNTs) composite. *J. Nanosci. Nanotechnol.* **7,** 1804–1809 (2007).
9 Akasaka, T., Watari, F., Sato, Y. & Tohji, K. Apatite formation on carbon nanotubes. *Mater. Sci. Eng. C* **26,** 675–678 (2006).
10 Tasis, D., Kastanis, D., Galiotis, C. & Bouropoulos, N. Growth of calcium phosphate mineral on carbon nanotube buckypapers. *Phys. Stat. Sol. (b)* **243,** 3230–3233 (2006).
11 Kongkanand, A., Kuwabata, S., Girishkumar, G. & Kamat, P. Single-wall carbon nanotubes supported platinum nanoparticles with improved electrocatalytic activity for oxygen reduction reaction. *Langmuir* **22,** 2392–2396 (2006).
12 Girishkumar, G., Vinodgopal, K. & Kamat, P. V. Carbon nanostructures in portable fuel cells: single-walled carbon nanotube electrodes for methanol oxidation and oxygen reduction. *J. Phys. Chem. B* **108,** 19960–19966 (2004).
13 Tajima, T., Sakata, W., Wada, T., Tsutsui, A., Nishimoto, S., Miyake, M. & Takaguchi, Y. Photosensitized hydrogen evolution from water using a single-walled carbon nanotube/fullerodendron/SiO_2 coaxial nanohybrid. *Adv. Mater.* **23,** 5750–5754 (2011).
14 Bäuerlein, E., Behrens, P. & Epple, M. Eds. *Handbook of Biomineralization* (Wiley-VCH, Weinheim, 2007).
15 Kato, T. Polymer/calcium carbonate layered thin-film composites. *Adv. Mater.* **12,** 1543–1546 (2000).
16 Kato, T., Sugawa, A. & Hosoda, N. Calcium carbonate-organic hybrid materials. *Adv. Mater.* **14,** 869–877 (2002).
17 Kato, T., Sakamoto, T. & Nishimura, T. Macromolecular templating for the formation of inorganic-organic hybrid structures. *MRS Bull.* **35,** 127–132 (2010).
18 Meldrum, F. C. & Cölfen, H. Controlling mineral morphologies and structure in biological and synthetic systems. *Chem. Rev.* **108,** 4332–4432 (2008).
19 Xu, A.-W., Ma, Y. & Cölfen, H. Biomimetic mineralization. *J. Mater. Chem.* **17,** 415–449 (2007).
20 Meldrum, F. C. Calcium carbonate in biomineralisation and biomimetic chemistry. *Int. Mater. Rev.* **48,** 187–224 (2003).
21 Imai, H., Oaki, Y. & Kotachi, A. A biomimetic approach for hierarchically structured inorganic crystals through self-organization. *Bull. Chem. Soc. Jpn.* **79,** 1834–1851 (2006).
22 Sommerdijk, N. A. J. M. & de Wirh, G. Biomimetic $CaCO_3$ mineralization using designer molecules and interfaces. *Chem. Rev.* **108,** 4499–4550 (2008).
23 Naka, K. Effect of dendromers on the crystallization of calcium carbonate in aqueous solution. *Top. Curr. Chem.* **228,** 141–158 (2003).
24 Naka, K., Tanaka, Y., Chujo, Y. & Ito, Y. The effect of an anionic starburst dendrimer on the crystallization of $CaCO_3$ in aqueous solution. *Chem. Comm.* **39,** 1931–1932 (1999).
25 Tanaka, Y., Nemoto, T., Naka, K. & Chujo, Y. Preparation of $CaCO_3$/polymer composite films via interaction of anionic starburst dendrimer with poly(ethylenimine). *Polmer. Bull* **45,** 447–450 (2000).
26 Naka, K., Kobayashi, A. & Chujo, Y. Effect of anionic 4.5-generation polyamidoamine dendrimer on the formation of calcium carbonate polymorphs. *Bull. Chem. Soc. Jpn.* **75,** 2541–2546 (2002).
27 Naka, K., Tanaka, Y. & Chujo, Y. Effect of anionic starburst dendrimers on the crystallization of $CaCO_3$ in aqueous solution: Size control of spherical vaterite particles. *Langmuir* **18,** 3655–3658 (2002).
28 Keum, D.-K., Naka, K. & Chujo, Y. Effect of anionic polyamidoamine dendrimers on the crystallization of calcium carbonate by delayed addition method. *Bull. Chem. Soc. Jpn.* **76,** 1687–1691 (2003).
29 Takaguchi, Y., Yanagimoto, Y., Tajima, T., Ohta, K., Motoyoshiya, J. & Aoyama, H. Photodimerization of anthracene having dendritic substituent within the vaterite crystal of $CaCO_3$. *Chem. Lett.* **31,** 1102–1103 (2002).
30 Talukdar, B., Takaguchi, Y., Yanagimoto, Y., Tsuboi, S., Ichihara, M. & Ohta, K. Fabrication and photocatalytic activity of fullerodendron/$CaCO_3$ composites. *Bull. Chem. Soc. Jpn.* **79,** 1983–1987 (2006).
31 Anderson, R. E. & Barron, A. R. Effect of carbon nanomaterials on calcium carbonate crystallization. *Main Group Chem.* **4,** 279–289 (2005).
32 Li, W. & Gao, C. Efficiently stabilized spherical vaterite $CaCO_3$ crystals by carbon nanotubes in biomimetic mineralization. *Langmuir* **23,** 4575–4582 (2007).
33 Ford, W. E., Yasuda, A. & Wessels, J. M. Microcrystalline composite particles of carbon nanotubes and calcium carbonate. *Langmuir* **24,** 3479–3485 (2008).
34 Holzinger, M., Vostrowsky, O., Hirsch, A., Hennrich, F., Kappes, M., Weiss, R. & Jellen, F. Sidewall functionalization of carbon nanotubes. *Angew. Chem. Int. Ed.* **40,** 4002–4005 (2001).
35 Hirsch, A. Functionalization of single-walled carbon nanotubes. *Angew. Chem. Int. Ed.* **41,** 1853–1859 (2002).
36 Tasis, D., Tagmatarchis, N., Georgakilas, V. & Prato, M. Soluble carbon nanotubes. *Chem. Eur. J.* **9,** 4000–4008 (2003).
37 Li, H., Cheng, F., Duft, A. D. & Adronov, A. Functionalization of single-walled carbon nanotubes with well-defined polystyrene by 'click' coupling. *J. Am. Chem. Soc.* **127,** 14518–14524 (2005).
38 Tasis, D., Tagmatarchis, N., Bianco, A. & Prato, M. Chemistry of carbon nanotubes. *Chem. Rev.* **106,** 1105–1136 (2006).
39 Karousis, N. & Tagmatarchis, N. Current progress on the chemical modification of carbon nanotubes. *Chem. Rev.* **110,** 5366–5397 (2010).
40 Britz, D. A. & Khlobystov, A. N. Noncovalent interactions of molecules with single walled carbon nanotubes. *Chem. Soc. Rev.* **35,** 637–659 (2006).
41 Byrne, M. T. & Gun'ko, Y. K. Recent advances in research on carbon nanotube–polymer composites. *Adv. Mater.* **22,** 1672–1688 (2010).
42 Moniruzzaman, M. & Winey, K. I. Polymer nanocomposites containing carbon nanotubes. *Macromolecules* **39,** 5194–5205 (2006).
43 Shen, Y., Skirtach, A. G., Seki, T., Yagai, S., Li, H., Möhwald, H. & Nakanishi, T. Assembly of fullerene-carbon nanotubes: Temperature indicator for photothermal conversion. *J. Am. Chem. Soc.* **132,** 8566–8568 (2010).
44 Nakashima, N., Tomonari, Y. & Murakami, H. Water-soluble single-walled carbon nanotubes via noncovalent sidewall-functionalization with a pyrene-carrying ammonium ion. *Chem. Lett.* **31,** 638–639 (2002).
45 Takaguchi, Y., Sako, Y., Yanagimoto, Y., Tsuboi, S., Motomoyushiya, J., Aoyama, H., Wakahara, T. & Akasaka, T. Facile and reversible synthesis of an acidic water-soluble poly(amidoamine) fullerodendrimer. *Tetrahedron Lett.* **44,** 5777–5780 (2003).
46 Takaguchi, Y., Tamura, M., Sako, Y., Yanagimoto, Y., Tsuboi, S., Uchida, T., Shimamura, K., Kimura, S., Wakahara, T., Maeda, Y. & Akasaka, T. Fullerodendron-assisted dispersion of single-walled carbon nanotubes via noncovalent functionalization. *Chem. Lett.* **34,** 1608–1609 (2005).
47 Levi, Y., Albeck, S., Brack, A., Weiner, S. & Addadi, L. Control over aragonite crystal nucleation and growth: An *in vitro* study of biomineralization. *Chem. Eur. J.* **4,** 389–396 (1998).
48 Homma, Y., Suzuki, S., Kobayashi, Y. & Nagase, M. Mechanism of bright selective imaging of single-walled carbon nanotubes on insulators by scanning electron microscopy. *Appl. Phys. Lett.* **84,** 1750–1752 (2004).
49 Vagenas, N. V., Gatsouli, A. & Kontoyannis, C. G. Quantitative analysis of synthetic carbonate polymorphs using FT-IR spectroscopy. *Talanta* **59,** 831–836 (2003).
50 Dresselhaus, M. S., Dresselhaus, G. & Jorio, A. in *Handbook of Nanophysics: Nanotubes and Nanowires* (ed. Sattiler, K. D.))Part 1, Ch. 7 I1–19 (CRC Press, Taylor & Francis, Boca Ratón, US, , 2011).
51 Kasselouri, V., Dimopoulos, G. & Parissakis, G. Effect of acetic and tartaric acid upon the thermal decomposition of $CaCO_3$. *Cem. Concr. Res.* **25,** 477–484 (1995).
52 Kasselouri, V., Dimopoulos, G. & Parissakis, G. Decomposition of $CaCO_3$ in the presence of organic acids. *Cem. Concr. Res.* **25,** 955–960 (1995).
53 Singh, N. B. & Singh, N. P. Formation of CaO from thermal decomposition of calcium carbonate in the presence of carboxylic acids. *J. Therm. Anal. Cal.* **89,** 159–162 (2007).
54 Bachilo, S. M., Balzano, L., Herrera, J. E., Pompeo, F., Resasco, D. E. & Weisman, R. B. Narrow (*n,m*)-distribution of single-walled carbon nanotubes grown using a solid supported catalyst. *J. Am. Chem. Soc.* **125,** 11186–11187 (2003).

Supplementary Information accompanies the paper on Polymer Journal website (http://www.nature.com/pj)